Deep-Sea Research I 89 (2014) 94–103

Contents lists available at ScienceDirect

Deep-Sea Research I

journal homepage: www.elsevier.com/locate/dsri

Particle flux characterisation and sedimentation patterns of protistan plankton during the iron fertilisation experiment LOHAFEX in the Southern Ocean

Friederike Ebersbach [a,b,*], Philipp Assmy [a,b,1], Patrick Martin [c,2], Isabelle Schulz [a,b], Sina Wolzenburg [b], Eva-Maria Nöthig [b]

[a] MARUM - Center for Marine Environmental Sciences, University of Bremen, Leobener Strasse, 28359 Bremen, Germany
[b] Alfred Wegener Institute for Polar and Marine Research, Am Handelshafen 12, 27570 Bremerhaven, Germany
[c] National Oceanography Centre, Southampton SO14 3 ZH, UK

ARTICLE INFO

Article history:
Received 18 May 2013
Received in revised form
10 April 2014
Accepted 15 April 2014
Available online 24 April 2014

Keywords:
Nano- and picoplankton
Export flux
Iron fertilisation
Protists
Sediment trap
Southern Ocean

ABSTRACT

The taxonomic composition and types of particles comprising the downward particle flux were examined during the mesoscale artificial iron fertilisation experiment LOHAFEX. The experiment was conducted in low-silicate waters of the Atlantic Sector of the Southern Ocean during austral summer (January–March 2009), and induced a bloom dominated by small flagellates. Downward particle flux was low throughout the experiment, and not enhanced by addition of iron; neutrally buoyant sediment traps contained mostly faecal pellets and faecal material apparently reprocessed by mesozooplankton. TEP fluxes were low, ≤ 5 mg GX eq. m^{-2} d^{-1}, and a few phytodetrital aggregates were found in the sediment traps. Only a few per cent of the POC flux was found in the traps consisting of intact protist plankton, although remains of taxa with hard body parts (diatoms, tintinnids, thecate dinoflagellates and foraminifera) were numerous, far more so than intact specimens of these taxa. Nevertheless, many small flagellates and coccoid cells, belonging to the pico- and nanoplankton, were found in the traps, and these small, soft-bodied cells probably contributed the majority of downward POC flux via mesozooplankton grazing and faecal pellet export. TEP likely played an important role by aggregating these small cells, and making them more readily available to mesozooplankton grazers.

1. Introduction

The downward flux of particulate organic carbon (POC) out of the surface ocean, known as the biological pump (Volk and Hoffert, 1985; De La Rocha, 2007), exerts an important control on atmospheric CO_2 concentrations (Parekh et al., 2006; Kwon et al., 2009). Although most of the sinking POC is remineralized in the upper few hundred metres, some sinks below the permanent thermocline and is removed from contact with the atmosphere for climatically-relevant time-scales (Lutz et al., 2002; Buesseler and Boyd, 2009; Kwon et al., 2009). The magnitude of the POC flux is strongly dependent on the nature of the particles that are exported from the surface, which is governed by the structure of the phytoplankton and grazer community in the surface and the mesopelagic (100–1000 m) (Boyd and Trull, 2007; Buesseler and Boyd, 2009).

However, even basic questions remain debated, such as which type of particles, and which phytoplankton taxa, contribute most to the flux out of the euphotic zone, and which have a greater tendency to pass through the mesopelagic zone without being remineralised. It is now appreciated that phytodetrital aggregates, not just zooplankton faecal pellets, are a key component of the particle flux (Turner, 2002). Export of phytodetrital aggregates is probably mediated by transparent exopolymer particles (TEP), which promote aggregation. However, few studies have measured downward TEP fluxes (Passow et al., 2001; Martin et al., 2011; Assmy et al., 2013). Moreover, an outstanding question concerns the degree to which the very small, ubiquitous nano- and picoplankton contribute to downward flux. The long-held view that only large-celled phytoplankton, such as diatoms, contribute directly to particle flux (Michaels and Silver, 1988) has recently been challenged based on results from modelling and from

Abbreviations: prot C, protist carbon; POC, particulate organic carbon; TEP, transparent exopolymer particles

* Corresponding author at: MARUM - Center for Marine Environmental Sciences, University of Bremen, Leobener Strasse, 28359 Bremen, Germany. Tel.: +49 4212186550.
E-mail address: friederike.ebersbach@gmx.net (F. Ebersbach).
[1] Present address: Norwegian Polar Institute, Fram Centre, 9296 Tromsø, Norway.
[2] Present address: Earth Observatory of Singapore, Nanyang Technological University, 50 Nanyang Avenue, Singapore 639798, Singapore.

http://dx.doi.org/10.1016/j.dsr.2014.04.007

biochemical and carbon isotopic analyses (Richardson and Jackson, 2007; Close et al., 2013). Our overall still poor understanding of the biological pump limits our ability to predict responses to environmental changes (Taucher and Oschlies, 2011).

The Southern Ocean consists largely of High-Nitrate-Low-Chlorophyll (HNLC) areas, where primary production is limited by iron (Fe) availability (Martin, 1990; Boyd et al., 2007). This has raised the question of whether enhancing Fe supply to the Southern Ocean would stimulate the biological pump and sequester anthropogenic CO_2 (Lampitt et al., 2008a; Smetacek and Naqvi, 2008).

Five artificial Fe fertilisation experiments have been carried out in the Southern Ocean: SOIREE (Boyd et al., 2000), SOFeX-N and -S (Coale et al., 2004), EisenEx (Assmy et al., 2007), EIFEX (Smetacek et al., 2012), and SAGE (Harvey et al., 2011). Further two studies examined naturally Fe fertilised waters downstream of Southern Ocean islands, CROZEX (Pollard et al., 2009) and KEOPS (Blain et al., 2007). Although carbon export at 200 m was enhanced during SOFeX, EIFEX, CROZEX and KEOPS (Coale et al., 2004; Salter et al., 2007; Blain et al., 2007; Smetacek at el., 2012), enhancement of deep export (>1000 m) was observed only during EIFEX and CROZEX (Pollard et al., 2009; Smetacek at el., 2012), although particle stocks during KEOPS were enhanced down to 400 m in fertilised relative to unfertilised waters (Jouandet et al., 2011). However, many artificial Fe fertilisation experiments were too short to follow the demise of Fe-induced blooms (Smetacek and Naqvi, 2008). The LOHAFEX experiment (*loha* means iron in Hindi) was hence designed to follow the build-up and demise of the bloom, and to fertilise an area large enough to minimise the effects of dilution with unfertilised waters (Smetacek and Naqvi, 2008).

This manuscript focuses on the contribution of intact cells of phytoplankton and protozooplankton to the downward carbon flux during LOHAFEX, and reports the TEP distribution in the water column and downward TEP fluxes.

2. Material and methods

2.1. Study area

LOHAFEX was conducted during austral summer in the Antarctic Polar Frontal Zone in the Atlantic Sector of the Southern Ocean (48°S and 15°W). A $\sim$300 km^2 patch in the centre of a cyclonic eddy was fertilised with 2 t of iron (as 10 t of $FeSO_4 \cdot 7H_2O$) on January 27 (d0) (Fig. 1), and marked with surface-tethered buoys equipped with GPS. Another 2 t of iron was applied 18 days later. Stations inside the patch (IN-stations) were distinguished from control stations outside the patch (OUT-stations) based on the photosynthetic quantum efficiency (Fv/Fm ratio) of phytoplankton, and concentrations of chlorophyll, pCO_2, and the inert tracer SF_6. The fertilised patch was studied for 39 days (27 January–6 March 2009), making LOHAFEX the longest iron fertilisation experiment to date.

2.2. Sediment traps

Funnel-shaped neutrally buoyant PELAGRA sediment traps (Lampitt et al., 2008b) were deployed at 200 and 450 m depth (Table 1). Multiple deployments of 1–6 days each were made throughout the experiment to collect as close to a contiguous record of particle flux as possible. Each trap has four separate collection funnels, each leading to a 500 mL Nalgene collection cup. Collection cups were programmed to open 18–24 h after deployment (by sliding under the funnel), and to close again before ascending to the surface.

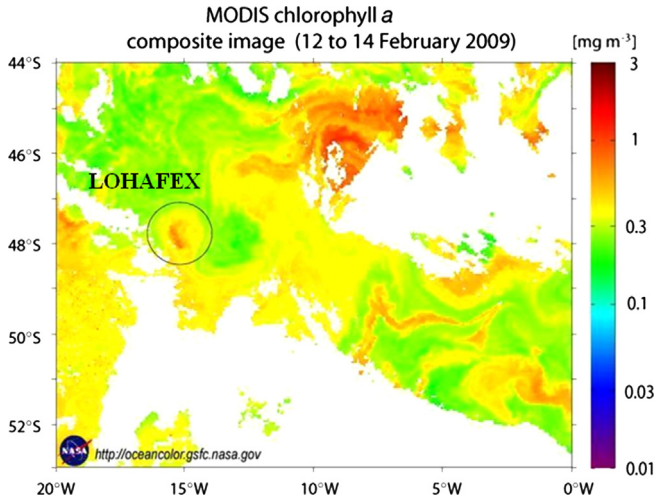

Fig. 1. Composite MODIS image of the LOHAFEX study area showing Chl *a* surface concentrations in the period 12–14 February. The iron induced bloom is encircled (its elongated form is just an "illusion" because the "circular" patch moved over the three days the MODIS image was assembled). Note the size of the much larger natural phytoplankton blooms in the northeast of the (artificial) LOHAFEX bloom for comparison.
Source: http://modis.gsfc.nasa.gov/.

Trap collection cups were filled prior to deployment with 2% borate-buffered formaldehyde in filtered (0.2 μm) seawater with NaCl added to 0.5%. Recovered samples were split on board using a rotary splitter, and splits for plankton counts were stored at 4 °C.

Polyacrylamide gels were deployed in some trap cups to preserve sinking particles intact. Gels were prepared prior to the cruise, and photographed on board after trap recovery following Ebersbach and Trull (2008). Particles identified in gels were classed as intact faecal pellets, reprocessed faecal material and phytodetritus (S 1). Faecal pellets (fp in S 1) were distinguished by a clearly-defined shape, owing to the membrane surrounding the pellet. Most pellets were cylindrical, but some were oval. Loose, very fluffy aggregates with no defined shape were classed as phytodetritus (pd in S 1). Particles that were more compact and with a better-defined shape than phytodetritus, but looser than faecal pellets, were classed as reprocessed faecal material (fm in S 1). We attribute such reprocessed material to coprorhexy and coprochaly of faecal pellets by copepods (Lampitt et al., 1990; Noji et al., 1991), which was apparently extensive during LOHAFEX (Martin et al., 2013).

2.3. Microscopic analyses and data processing

The sinking material collected with PELAGRA traps was examined using inverted light and epifluorescence microscopy (Axiovert 135, 200; Zeiss, Oberkochen, Germany) following the method of Throndsen (1995). Subsamples of 10 or 50 mL, depending on the density of the material, were settled in sedimentation chambers (Hydrobios; Kiel, Germany) for 48 h. Protists were identified and a minimum of 500 cells counted at either 100×, 200×, or 400×, depending on cell size. Depending on their abundance, cells were counted in transects, quarter, half, or whole chambers, and identified to species level where possible.

The biovolume of each taxon was estimated according to Hillebrand et al. (1999) by measuring 10–20 individuals per taxon at 400× magnification. Biovolumes were converted into carbon content after Menden-Deuer and Lessard (2000). Using the taxon-specific carbon content per cell, and the abundance of each taxon in the sediment trap samples, we calculated the carbon flux contributed by each taxon (in mg C m^{-2} d^{-1}). This is referred to below as protist carbon (prot C) flux.

Table 1
PELAGRA trap deployments. While trap #2 was only for gel deployments, traps #9 and #11 delivered gels and bulk samples for biogeochemical analysis, the remaining traps delivered bulk samples only.

#	Collection days	Depth (m)	Patch	Gels	Start position	End position
1	d0–d2	210	IN		48.024°S, 15.811°W	47.872°S, 15.881°W
2	d0–d2	450	IN	1, 2, 3	48.027°S, 15.802°W	47.885°S, 15.884°W
3	d10–d15	440	prob. IN		47.732°S, 15.125°W	47.849°S, 15.470°W
4	d13–d15	200	prob. IN		47.895°S, 15.265°W	47.799°S, 15.519°W
5	d17–d21	470	OUT		47.503°S, 15.441°W	47.479°S, 14.886°W
6	d22–d26	440	IN		47.655°S, 15.595°W	47.586°S, 14.561°W
7	d23–d28	440	IN		47.351°S, 15.417°W	47.894°S, 14.425°W
8	d24–d29	430	OUT		47.300°S, 15.556°W	48.385°S, 14.626°W
9	d26–d27	230	OUT	4, 5	47.514°S, 15.451°W	48.373°S, 14.754°W
10	d29–d33	460	IN		48.086°S, 14.467°W	48.979°S, 15.135°W
11	d34–d37	440	IN	6	48.796°S, 15.237°W	49.041°S, 15.285°W

Prot C comprised both phyto- and protozooplankton. Amongst the phytoplankton, we distinguished diatoms, flagellates, silicoflagellates, coccoid cells, and dinoflagellates. All cells with a flagellum were classed as flagellates. We did not distinguish between auto- and heterotrophic flagellates but between size classes (2.5–5, 5–10, and 10–20 μm) for the purpose of prot C calculation. Coccoid cells were defined as circular autotrophic cells up to 2 μm in size that lacked flagella. Protozooplankton was divided into dinoflagellates, ciliates, foraminifera, radiolaria, and heliozoa. Dinoflagellates were not differentiated into auto- and heterotrophic but into thecate and athecate taxa. Where possible, we distinguished between different species of diatoms, flagellates, and dinoflagellates; all taxa identified are listed in Supplementary Table 1.

For diatoms and tintinnid ciliates (tintinnids), we also enumerated intact empty and broken frustules and intact empty and damaged loricae according to Assmy et al. (2007, 2013). To enumerate broken frustules, only fragments consisting of >50% of the frustule were counted to prevent double-counting broken frustules. Damaged loricae were either crushed or there were parts missing. Empty diatom frustules can result from natural cell death, viral infection, parasite infestation, and protozoan or metazoan grazing, while broken frustules are mainly due to copepod grazing (Assmy et al., 2007; Assmy et al., 2013). Empty tintinnid loricae can result either from disruption of the delicate ciliate cell during fixation, or from the same mortality factors as those for empty diatom frustules except metazoan grazing. Due to the stiff, leathery consistency of tintinnid loricae it is mainly copepod grazing that results in damaged specimens (Assmy et al., 2013). Although intact empty and broken diatom frustules contain very little or no carbon, we calculated their equivalent carbon content as for full cells of each species to yield a ratio of full to empty and broken frustules (F:EB). This ratio illustrates the role of mortality factors versus sinking of intact cells for the total diatom flux. Only the carbon content of full diatom cells was used to calculate total prot C flux and the relative contribution of diatoms to C flux. The lorica carbon content on the other hand was estimated to account on average for 10% of the total carbon content of tintinnids. This estimate is considerably lower than the lorica carbon content given by Gilron and Lynn (1989) because the loricae of the dominant species, in particular *Acanthostomella norvegica*, were very thin (1–2 μm) and already partly digested.

2.4. TEP analyses

TEP were measured both in the sediment trap samples and in the water column. Water samples of 250 mL were collected from the upper 500 m with Niskin bottles attached to a CTD rosette, and were processed in duplicate within a few hours of collection following Passow and Alldredge (1995). Samples were filtered onto 0.4 μm polycarbonate filters, stained with Alcian blue and stored at −20 °C in sealed polycarbonate tubes. TEP in sediment trap samples were stained according to Passow et al. (2001).

Stained filters were then dissolved in 80% H_2SO_4, and the absorbance at 787 nm was measured on a Pharma Spec UV-1700 spectrophotometer. The Alcian blue solution was calibrated against Gum Xanthan and TEP expressed as Gum Xanthan equivalents (μg GX eq. L^{-1}).

Water column TEP inventories were integrated from 0 to 100, 200, and 500 m. TEP fluxes, in mg GX eq. m^{-2} d^{-1}, were calculated from the TEP content of trap material.

3. Results

3.1. Summary of physical and biological developments following fertilisation

The fertilised patch rotated for four and a half weeks inside the closed eddy core and was then filamented towards the end of the experiment due to entrainment of the LOHAFEX eddy by a neighbouring anti-cyclone. The fertilised patch could be tracked for 39 d post-fertilisation, making LOHAFEX the longest iron fertilisation experiment to date. Trap trajectories mirrored the circulation in the upper 200 m, determined by shipboard ADCP surveys and revealed by the drift of the buoys, indicating a vertically coherent circulation down to at least 450 m (Martin et al., 2013). Most probably, the traps thus collected material sinking down from immediately above, allowing a reliable distinction between IN- and OUT-patch traps.

Upon Fe addition, Fv/Fm increased from initially 0.33 to 0.4–0.5 throughout the experiment, while nitrate decreased from 20 to 17.5 μmol L^{-1}, and $Si(OH)_4$ remained low at 0.6–1.6 μmol L^{-1}. Chl *a* standing stocks doubled after fertilisation to ~80 mg m^{-2}, but remained ~40 mg m^{-2} outside the patch (Schulz et al., in prep.). ^{14}C primary production peaked at 130 mmol C m^{-2} d^{-1} inside the patch, but remained <80 mmol C m^{-2} d^{-1} outside (M. Gauns, personal communication). Net community production (NCP) rose after fertilisation, averaging 21 mmol m^{-2} d^{-1} ± 20% inside the patch, but was 0 mmol m^{-2} d^{-1} outside (Martin et al., 2013).

Non-diatom phytoplankton, mostly unidentified flagellates and coccoid cells, made up the bulk of protist plankton, while diatoms, dinoflagellates, and *Phaeocystis antarctica* accounted for <5%, 6%, and 10% of protist plankton inside the patch, respectively (Fig. 2). The community composition was very similar outside the patch, and did not change much over time (Schulz et al., in prep.). Although bacterial production, estimated by thymidine and leucine

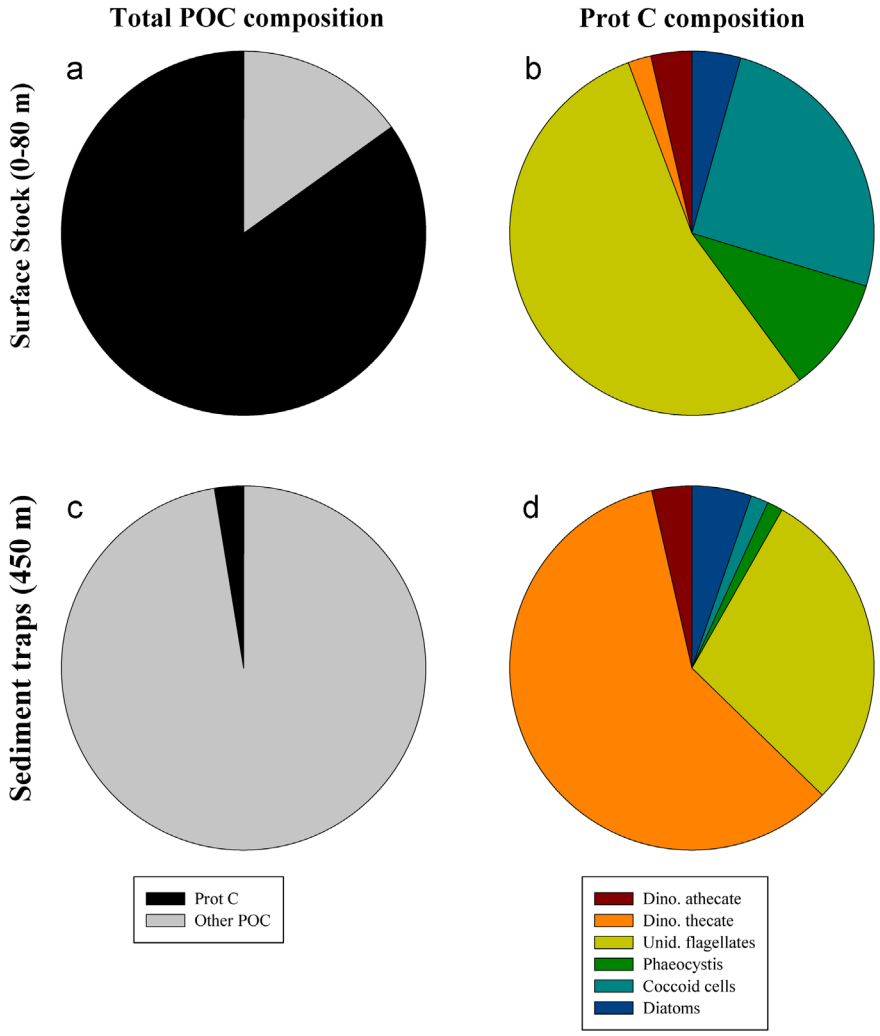

Fig. 2. Contribution of total protist carbon (prot C) to total POC (a and c), and composition of prot C (b and d) inside the patch – showing the large differences between surface standing stock (upper graphs) and flux (lower graphs). Surface data are averaged over all IN stations (integrated over the upper 80 m), and flux data show averages of 450 m deep IN deployments of sediment traps. Within the composition of prot C, thecate and athecate dinoflagellates, unidentified flagellates, *P. antarctica*, coccoid cells and diatoms are distinguished.

uptake, roughly doubled inside the patch thecomposition and abundance of the bacterial and archaeal community stayed remarkably constant throughout the experiment (Thiele et al., 2012). Stocks of protozooplankton and copepods <1 mm (including all naupliar and copepodite stages as well as adults of *Oithona* spp.) also stayed relatively stable inside and outside the patch (IN: 253 ± 66 mg C m^{-2}, OUT: 262 ± 98 mg C m^{-2}; integrated over the upper 80 m) (Schulz et al., in prep.). While stocks of copepods >1 mm, dominated by *Calanus simillimus*, were in the same order of magnitude IN and OUT but quite variable ($\sim 1700 \pm 1000$ mg C m^{-2}; integrated over the upper 200 m) (Mazzocchi et al., in prep.). Grazing rates of *C. simillimus* were especially high, with faecal pellet production rates implying grazing of $>30\%$ on average of NCP (range 0.7–240%) (Gonzalez et al., in preparation).

Downward POC fluxes were low throughout the experiment and did not differ between fertilised and unfertilised waters (Martin et al., 2013): PELAGRA traps caught mostly <12 mg POC m^{-2} d^{-1} at both 200 m and 450 m, while export at 100 m as diagnosed from ^{234}Th profiles was 75 mg C m^{-2} d^{-1}.

3.2. Flux characteristics from polyacrylamide gels

Numerous gels were deployed, but owing to technical problems with the traps only six were recovered successfully: three at the start and one at the very end of the experiment inside the patch (450 m), and two outside the patch at the end of the experiment (200 m) (Table 1). Moreover, unlike in studies using cylindrical sediment traps (Ebersbach and Trull, 2008; Ebersbach et al., 2011), the particles collected here may have been altered while travelling down the collection funnel. Most particles were deposited in a circle (S 2), indicating that they moved down the funnel instead of sinking undisturbed into the gel. The results must hence be interpreted with caution. Nevertheless, the gels indicated that particle flux consisted predominantly of faecal pellets and reprocessed faecal material, while fragile phyto-detrital aggregates were rare (Fig. 3). No major changes in the contribution by different particle classes were evident after fertilisation, nor differences between IN and OUT patch (Fig. 3).

3.3. Protist carbon (prot C) fluxes

Since there were only three 200 m traps, yielding samples very similar in composition to those from 450 m (Table 2), we focus here on results from 450 m traps.

Total prot C fluxes were very low, always <0.9 mg m^{-2} d^{-1}, and accounted for $<10\%$ of total POC flux (Figs. 2, 4; Table 2). Prot C fluxes were composed of diatoms, unidentified flagellates, autotrophic coccoid cells, *P. antarctica*, and thecate and athecate

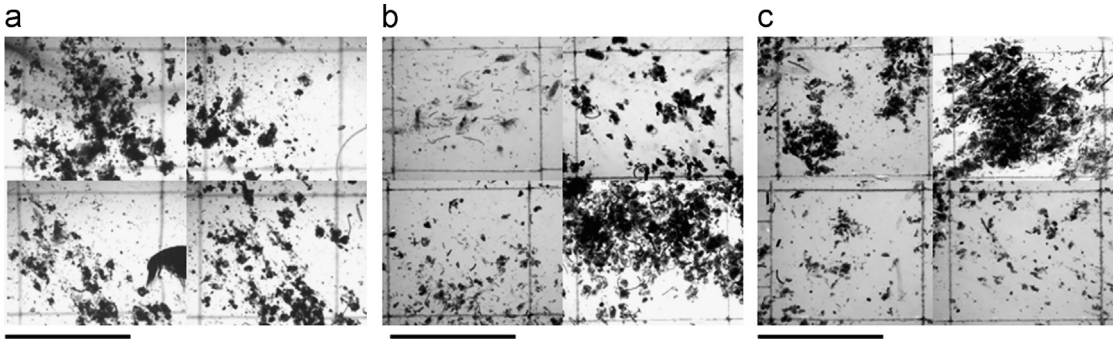

Fig. 3. Detailed images of the gels as they were obtained during LOHAFEX: (a) Gel 1–3 (IN, parallel samples, d0–d2), (b) Gel 4/5 (OUT, parallel samples, d26), and (c) Gel 6 (IN, d34). See Table 1 for deployment details. The majority of the collected particles appear to be of faecal origin; in the beginning the material seems to be more compact (a), while at the end more intact (and degraded) faecal pellets and reprocessed material were found (b), (c). Note that the proto-zooplankton almost disappeared in Gel 4–6 from the second half of the experiment. (Scale bar: 1 cm).

Table 2
Protist C (prot C) flux and surface standing stock (integrated over 80 m) of diatoms, flagellates, coccoid cells and dinoflagellates. Standing stock represents the average over all IN or all OUT stations.[a]

PELAGRA trap	***Diatoms***		***Unidentified flagellates***		***Phaeocystis antarctica***		***Coccoid cells***	
	% of POC flux	*% of POC surf. stock*	*% of POC flux*	*% of POC surf. stock*	*% of POC flux*	*% of POC surf. stock*	*% of POC flux*	*% of POC surf. stock*
200 m								
# 1*(IN), d0–d2*	0.52	4.00	1.06	50.34	0.00	9.47	0.04	23.45
# 4 *(IN), d13–d15*	0.36	4.00	1.22	50.34	0.06	9.47	0.08	23.45
# 9 *(OUT), d26–d27*	0.25	3.74	1.85	49.73	0.07	8.78	0.11	16.35
450 m *(IN)*								
# 3, *d10–d15*	0.20	4.00	0.37	50.34	0.05	9.47	0.01	23.45
# 6, *d21–d26*	0.14	4.00	0.53	50.34	0.01	9.47	0.02	23.45
# 7, *d23–d28*	0.05	4.00	0.19	50.34	0.01	9.47	0.01	23.45
# 10, *d28–d33*	0.14	4.00	0.96	50.34	0.06	9.47	0.06	23.45
# 11, *d33–d37*	0.24	4.00	2.15	50.34	0.07	9.47	0.12	23.45
450 m *(OUT)*								
# 5, *d17–d21*	0.87	3.74	1.32	49.73	0.27	8.78	0.04	16.35
# 8, *d24–d29*	0.43	3.74	0.70	49.73	0.01	8.78	0.05	16.35

Dinoflagellates						***Total prot C***		***Total POC***
Thecate		*Athecate*		*Total*				
% of POC flux	*% of POC surf. stock*	*% of POC flux*	*% of POC surf. stock*	*% of POC flux*	*% of POC surf. stock*	*% of POC flux*	*% of POC surf. stock*	***Flux*[b] mg C m^{-2} d^{-1}**
12.06	1.90	0.72	3.36	12.77	5.26	14.40	**92.51**	**5.56**
1.75	1.90	0.13	3.36	1.88	5.26	3.53	**92.51**	**4.78**
0.74	1.18	0.17	3.16	0.91	4.34	3.12	**82.94**	**28.39**
5.66	1.90	0.22	3.36	5.87	5.26	6.45	**92.51**	**8.44**
1.36	1.90	0.06	3.36	1.41	5.26	2.11	**92.51**	**9.18**
0.14	1.90	0.02	3.36	0.16	5.26	0.41	**92.51**	**22.96**
0.46	1.90	0.10	3.36	0.55	5.26	1.72	**92.51**	**12.82**
2.52	1.90	0.16	3.36	2.67	5.26	5.18	**92.51**	**12.85**
3.85	1.18	1.14	3.16	4.99	4.34	7.22	**82.94**	**2.83**
1.39	1.18	0.10	3.16	1.48	4.34	2.66	**82.94**	**10.97**

BSi			***TEP***
Flux [b] mg Si m^{-2} d^{-1}	*POC:Bsi* mol:mol		*Flux* mg GX eq m^{-2} d^{-1}
2.38	5.47		0.00
0.56	19.84		5.14
2.89	22.97		4.26
4.41	4.48		1.36
4.50	4.78		0.03
8.44	6.37		0.00
3.00	10.01		2.24
2.31	13.04		0.78
1.68	3.95		1.83
3.16	8.13		2.61

[a] Total POC for standing stock is the sum of protist C, bacteria C and copepods (<1 mm) C from Schulz et al. (in prep.).
[b] Total POC and BSi fluxes from PELAGRA traps (Martin et al., 2013).

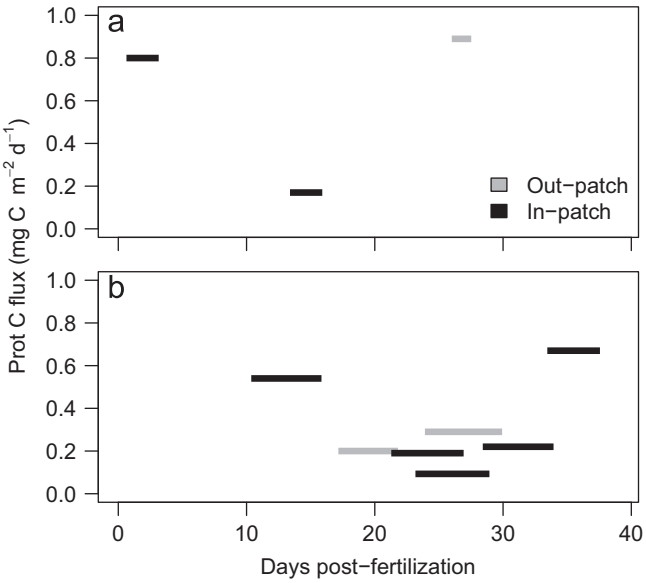

Fig. 4. Total protist carbon (prot C) flux determined from PELAGRA trap samples: development of IN and OUT fluxes at (a) 200 and (b) 450 m. IN and OUT stations are labelled in the graphs.

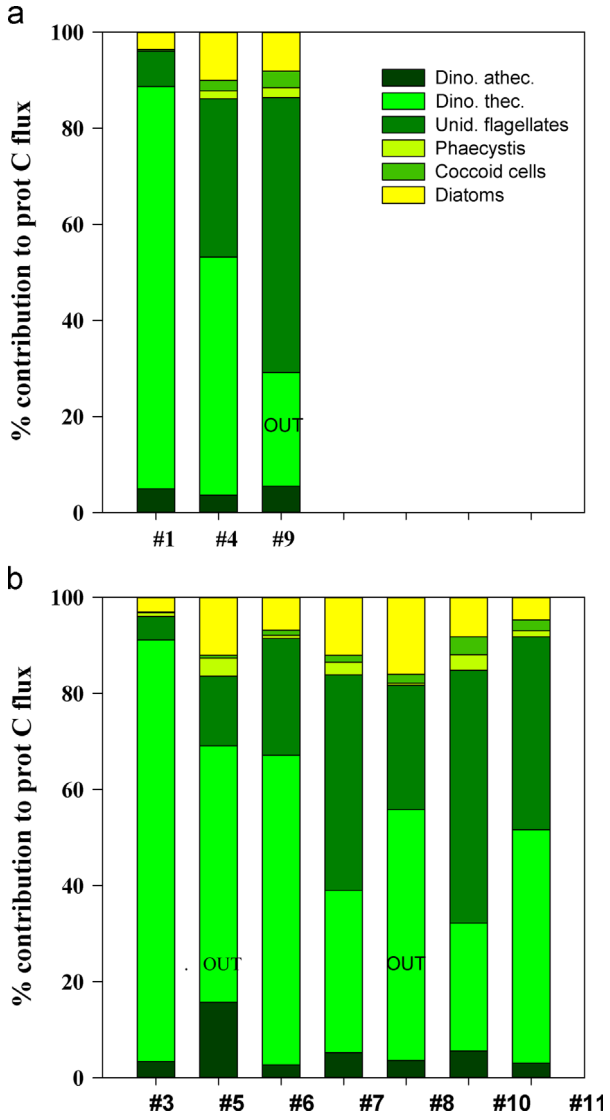

Fig. 5. Relative protist carbon (prot C) flux of the C flux carrying groups: thecate and athecate dinoflagellates, unidentified flagellates, *P. antarctica*, coccoid cells and diatoms over the course of the experiment at (a) 200 and (b) 450 m. OUT stations are labelled in the graphs; see Table 1 for deployment details of the sediment traps.

dinoflagellates. Tintinnids and foraminifera were present only as empty or damaged/broken individuals, and the majority of diatom frustules were broken. All other taxa were present at very low abundances.

In contrast to the prot C standing stock in the surface, which was dominated by flagellates and coccoid cells, the prot C in the sediment traps was dominated by thecate dinoflagellates and flagellates, with the other taxa contributing a similar proportion to the surface stock (Fig. 2). However, these proportions varied strongly over time: while thecate dinoflagellates contributed almost all prot C early on, their relative contribution declined in favour of flagellates (Fig. 5).

Concomitantly, we observed marked increases in the equivalent C flux of empty and broken diatom frustules (Fig. 6), even though total biogenic silicon (BSi) flux if anything decreased slightly during this period (Table 2). Moreover, POC fluxes of empty and damaged tintinnid loricae also increased (Supplementary Table 3), indicating the importance of grazing during LOHAFEX. Likewise, the vast majority of foraminiferan tests were empty (Supplementary Table 4), and some of these showed signs of grazing, such as broken spines and/or tests (Fig. 7).

3.4. TEP concentrations in the water column and TEP flux

TEP concentrations were quite low and decreased strongly with depth, but remained steady over time and were very similar inside and outside the patch (Fig. 7; Table 3). Depth-integrated TEP over the upper 100 m was <10 g GX eq. m^{-2} (Table 3). TEP and Chl *a* in the surface layer were not correlated ($R^2=0.15$, $p=0.28$).

TEP fluxes as caught in the sediment traps were very low throughout the experiment (always ≤ 5 mg GX eq. m^{-2} d^{-1}), and showed no marked temporal trends or IN versus OUT patch differences (Table 2).

4. Discussion

4.1. Sediment trap collections

We cannot prove beyond doubt that the traps collected particles from only inside or only outside of the fertilised patch. However, a ship-board ADCP showed that the surface circulation was homogenous down to at least 200 m, and the trajectories of all traps closely reflected the surface flow (Martin et al., 2013). Given such an apparently consistent circulation from the surface down to the depth of the traps, it is most likely that they did collect particles derived from a relatively small area of surface water not far from the trap location. It is therefore unlikely that trap collections were strongly biased by particles originating from far away.

4.2. Composition of the flux

While intact protists comprised the bulk of surface POC, as found generally in the open ocean (Martiny et al., 2013), direct sinking of intact cells (prot C) contributed only a very minor fraction of the downward POC flux below 200 m (Fig. 2; Table 2). This is in sharp contrast to mass sinking events after diatom blooms, in which the majority of downward POC flux may be contributed by intact cells or resting stages of a subset of diatom species (Assmy et al., 2013; Rynearson et al., 2013). The highest prot C contribution to POC flux during LOHAFEX was found at the

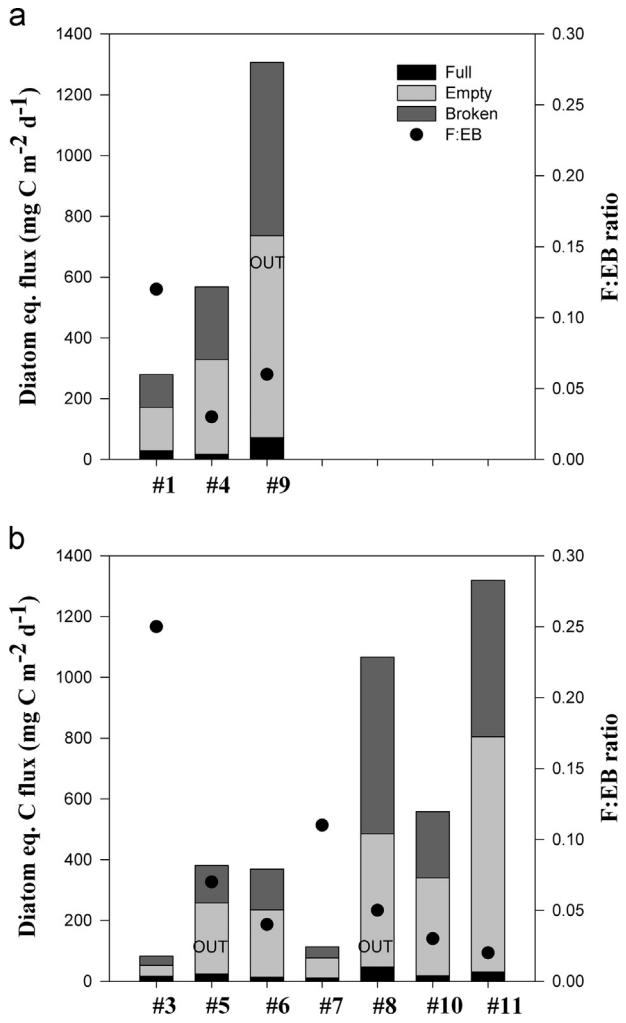

Fig. 6. Diatom POC flux (full frustules) and equivalent C flux (empty and broken frustules) at (a) 200 m, and (b) 450 m over the course of the experiment. OUT stations are labelled in the graphs; see Table 1 for deployment details of the sediment traps. On the 2nd y-axis the ratio of full to empty and broken frustules (F:EB ratio) is given for each trap sample.

start (Table 2), reflecting pre-fertilisation particle export (^{234}Th was already depleted at Day 0 (Martin et al., 2013)).

The taxonomic composition of the prot C flux differed from that found in the surface, notably in the high proportion of thecate dinoflagellates and the presence of empty theca (Figs. 2, 5; Table 2). Intact diatoms did not contribute notably more to prot C fluxes than to the standing stock, and although intact flagellates contributed less to prot C flux than to the standing stock, they nevertheless contributed nearly a third of prot C flux (Fig.2; Table 2). Even intact coccoid cells <2 μm were found in the trap (Table 2), clearly showing that small coccoid cells and flagellates can contribute as intact cells to the biological pump, without needing to pass through the microbial loop. This adds direct observational evidence to previous studies based on modelling (Richardson and Jackson, 2007) and on the biochemical and isotopic composition of suspended particles in the mesopelagic (Close et al., 2013). However, the low contribution of prot C to total downward POC flux (Fig. 2; Table 2), and the scarcity of phytodetritus in the gels (Fig. 3), indicate that direct aggregation and sinking of any protist classes was not a significant pathway for POC export.

Instead, the predominance of faecal pellets and disintegrating (reprocessed) faecal material (Fig. 3) points to mesozooplankton grazing as the primary vector for downward flux in the low-flux LOHAFEX system. The importance of mesozooplankton grazing for export of small-celled phytoplankton was highlighted by Wilson and Steinberg (2010), who reported the wide-spread presence of cyanobacterial aggregates in copepod guts. Likewise, Waite et al. (2000) reported intact picoplankton cells embedded within organic aggregates including faecal material, though only comprising $\leq 0.15\%$ of downward POC flux. Thus, the recognisable prot C in our sediment traps probably represents primarily the minor fraction that survived gut passage intact, and was then liberated from disintegrating faecal pellets in the traps. Flagellates and coccoid cells are far less distinct than diatom frustules, tintinnid loricae or dinoflagellate thecae (Table 2), and they would have been missed if embedded in larger particles. Their contribution might hence have been under-estimated, although our conclusion that intact protist cells contributed only a small proportion of POC flux is unaffected.

Increased particle disintegration could explain the apparent increase over time in empty and broken diatom frustules, empty and damaged tintinnid loricae, and in flagellate contribution to prot C – while no similar increase was found in total BSi flux (Table 2). It therefore seems likely that later traps contained a greater proportion of more strongly disintegrating faecal material, indicating more intense reprocessing of faecal pellets later in the experiment. The decrease of faecal pellets with depth, and the concomitant increase in unrecognisable detritus particles observed in PA gels points strongly to intense reprocessing of faecal pellets (Martin et al., 2013).

That the majority of diatom frustules and foraminifera were empty or broken (Fig.6, Supplementary Table 4), and all tintinnid loricae empty or damaged (Supplementary Table 3), clearly points to mesozooplankton grazing as the primary route for particle flux. While empty loricae might be caused by the detachment of the ciliate cell during sample fixation, no such detached ciliates were found in the trap, suggesting that the cells were grazed at the surface. Damaged loricae, in contrast, can only be explained by deformation of the tough, leathery lorica by crustacean grazing, as is the case for broken diatom frustules and foraminiferan tests. However, even though these protistan taxa with hard body parts leave recognisable remains even after crustacean grazing, their empty, broken and damaged hard parts still did not vastly dominate the sediment trap samples (Fig. 7). A large fraction of the total POC flux was therefore most likely derived from small cells rendered unrecognisable by mesozooplankton grazing, supporting the idea that nano- and picoplankton can contribute a significant proportion of the low downward particle fluxes out of "retention" systems (Wassmann, 1998) with high grazing pressure, such as LOHAFEX.

The very low proportion of full diatom cells compared to empty and broken frustules in the trap samples (Fig. 6) underscores the role of certain diatoms as "silica sinkers" in the Southern Ocean. This is particularly so for *Fragilariopsis kerguelensis*, the most abundant diatom species in the traps, and the one with the lowest F:EB ratio of the three most abundant diatom species (Supplementary Table 2). During the iron fertilisation experiment EIFEX, *F. kerguelensis* was also primarily responsible for silica export in form of empty frustules, rather than carbon export, which was enhanced due to mass sinking of other diatom species (Assmy et al., 2013).

4.3. Role of TEP for export processes

TEP concentrations were relatively low (Table 3; Fig. 8), although TEP concentrations even within the Southern Ocean have been reported to range from 10 to 2000 μg GX eq. L^{-1} (Passow et al., 1995; Hong et al., 1997; Corzo et al., 2005; Ortega-Retuerta et al., 2009). TEP fluxes in the sediment traps were also low (Table 2)

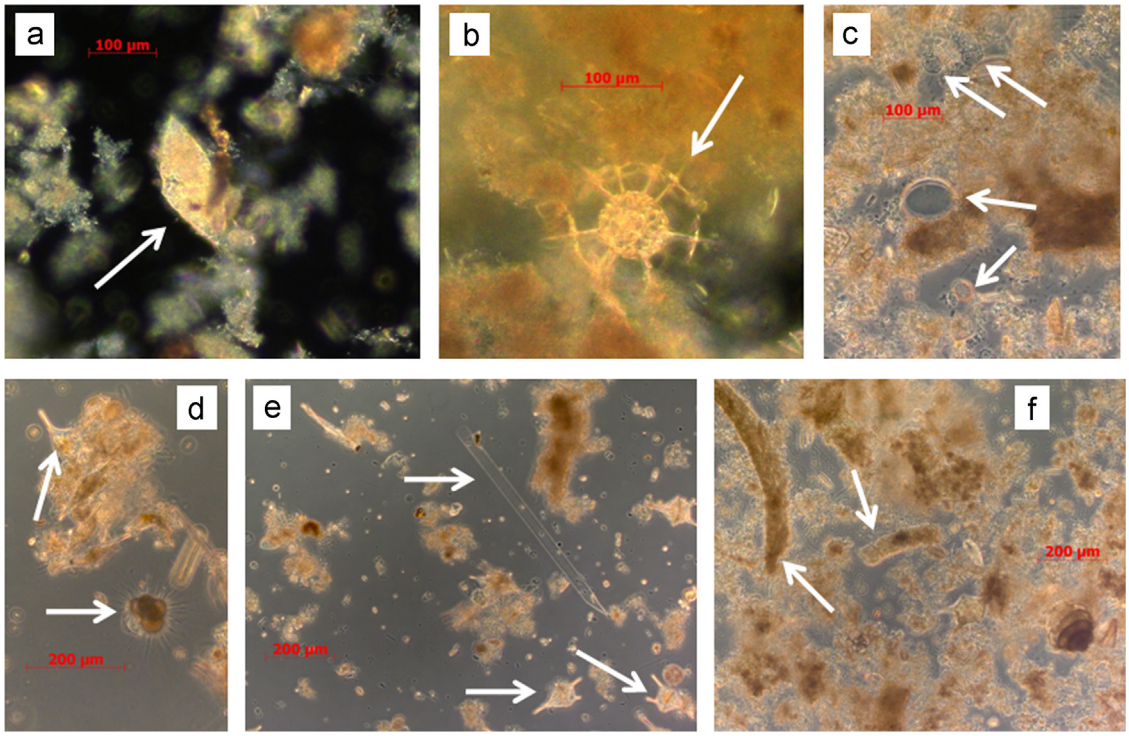

Fig. 7. Images showing the flux composition as examined with the microscope (from bulk sediment trap samples; a, b, c, f: 450 m; e, d: 200 m): (a) dinoflagellate *Gyrodinium* sp. and reprocessed faecal material and (loose) phyto-detritus, (b) broken radiolaria embedded in reprocessed faecal matter, (c) empty tintinnid loricae incorporated in reprocessed faecal material and phyto-detrital aggregates, (d) foraminifera with broken spines and dinoflagellate *Ceratium pentagonum* incorporated in reprocessed faecal material, (e) broken frustules of *Rhizosolenia* sp., thecae of *C. pentagonum*, and reprocessed faecal matter and phyto-detritus, and (f) reprocessed faecal material, phyto-detrital aggregates and recognisable individual faecal pellets.

Table 3
TEP concentration in the water column (in GX eq).

Day	*Chl a*[a]	*TEP in the water column*					
	Surface (10 m) ($\mu g\ L^{-1}$)	*surface* (10 m) ($mg\ m^{-3}$)	100 m $mg\ m^{-3}$	500 m $mg\ m^{-3}$	100 m (int.[b]) $g\ m^{-2}$	200 m (int.)[b] $g\ m^{-2}$	500 m (int.)[b] $g\ m^{-2}$
IN							
*d*0	0.48	88.06 ± 0.73	66.38 ± 4.40	55.30 ± 2.72	7.70	14.04	31.38
*d*4	0.87	91.49 ± 3.88[a]	61.25 ± 5.24	-	8.07	14.18	-
*d*9	1.20	86.29 ± 9.76	74.93 ± 12.17	62.92 ± 3.02	7.96	14.78	33.44
*d*12	0.84	90.77 ± 4.08	68.20 ± 5.01	59.42 ± 0.39	8.28	15.04	34.02
*d*18	1.06	93.31 ± 1.34	73.62 ± 1.85	-	8.66	15.31	-
*d*24	1.20	95.14	69.09 ± 1.22	66.81 ± 2.97	8.58	15.35	35.30
*d*33	0.94	75.13 ± 15.08	67.73 ± 1.41	59.56 ± 3.35	7.17	13.60	31.68
*d*36	0.82	83.95 ± 3.76	65.58 ± 5.47	61.32 ± 3.40	5.79	14.02	32.68
OUT							
*d*16	0.71	89.38 ± 6.76	64.44 ± 2.23	62.36 ± 0.51	8.09	14.82	34.27
*d*22	0.62	86.56 ± 7.45	70.81 ± 2.63	65.54 ± 2.06	8.27	15.18	35.15
*d*35	0.53	74.82 ± 0.15	69.28	63.21 ± 3.55	7.32	13.98	33.05

[a] Chl *a* measurement in the water column at 10 m (unpubl. data M. Gauns).
[b] TEP concentration integrated over the water column.

compared to fluxes of ~100 mg GX eq. $m^{-2}\ d^{-1}$ reported during collapse of a North Atlantic diatom bloom (Martin et al., 2013) and a time-series off California (Passow et al., 2001). However, 0–100 m TEP stocks during LOHAFEX were in a similar range as 2–8 g GXeq. m^{-2} reported during EIFEX (Assmy et al., 2013), at the end of which a mass sinking event of diatom aggregates was observed (Smetacek et al., 2012). Absolute TEP values should be compared with caution, since subtle differences in standard preparation and sampling protocols between studies could introduce systematic biases. However, as TEP comprise a potentially broad group of polysaccharides, TEP measured in different locations or at different times might differ physically and chemically such as to affect aggregation and downward flux differently. Neither downward flux nor TEP stocks varied much throughout LOHAFEX (Tables 2, 3); in contrast, towards the end of EIFEX the TEP stock more than doubled. During EIFEX, TEP certainly facilitated aggregation but the main binding agent seemed to have been autolysed cytoplasm released after cell death, as has been reported for the giant diatom *Coscinodiscus wailesii* (Armbrecht et al. 2014).

Neither POC and TEP fluxes, nor prot C and TEP fluxes were correlated (R^2=0.01, p=0.80 and R^2=0.01, p=0.82, respectively), again suggesting that direct export of TEP-rich aggregates was low, although the lack of large changes in POC flux may be responsible for the lack of correlation.

TEP flux during LOHAFEX may have been largely due to mesozooplankton grazing on detritus aggregates in the surface.

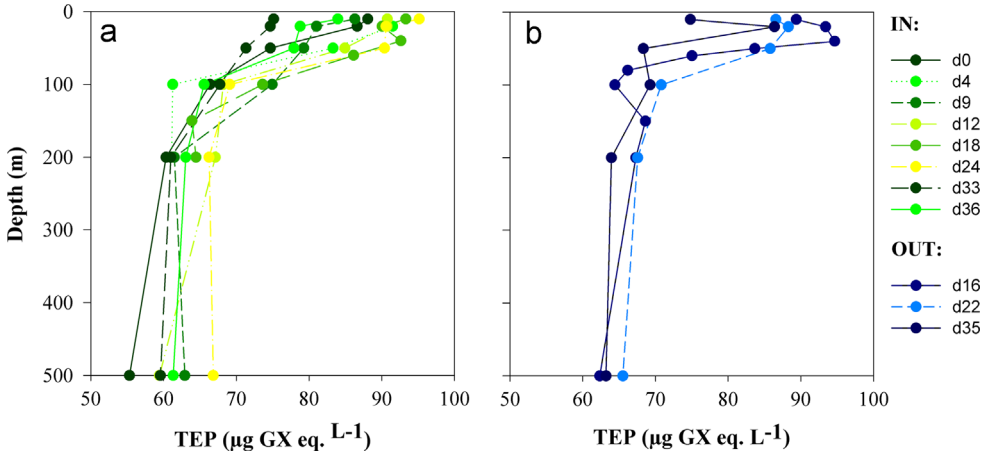

Fig. 8. TEP distribution in the upper 500 m of the water column: profiles (a) IN, and (b) OUT.

Mesozooplankton can ingest TEP (Passow and Alldregde, 1999; Ling and Alldregde, 2003) and aggregates of cells otherwise too small to feed on (Wilson and Steinberg, 2010), and while no large-scale TEP-mediated aggregation and mass sinking event was observed during LOHAFEX, TEP may have been critical to make the pico- and nanoplankton that dominated the bloom more accessible to crustacean grazers, thus indirectly mediating downward POC flux.

5. Conclusions

LOHAFEX resulted in a moderate bloom dominated by pico- and nanoplankton, especially small flagellates, which acted as a retention system with high grazing pressure by copepods. The low downward particle fluxes we observed were dominated by faecal material, which appeared to be reprocessed by copepods engaging in coprorhexy and coprochaly. Although sinking particles contained hard parts of large-celled taxa, mostly showing signs of grazing damage, these groups contributed a small proportion of downward POC flux. Instead, a large fraction of the POC flux was most likely contributed by pico- and nanoplankton, and indeed many individuals of these small-celled taxa were still recognisable in sinking particle samples recovered at 450 m depth. Although TEP concentrations were low and of similar magnitude as observed during EIFEX, TEP-mediated aggregation and mass sinking of intact phytoplankton cells were not significant pathways for export during LOHAFEX. Instead, TEP possibly enabled mesozooplankton grazing on small phytoplankton, promoting their export via faecal pellets.

Acknowledgements

We thank LOHAFEX co-chief scientists Victor Smetacek and Wajih Naqvi, and the captain and crew of *RV Polarstern*. Kevin Saw prepared and deployed PELAGRA traps. We are grateful to Uta Passow, Dieter Wolf-Gladrow and Ulrich Bathmann for thoughtful discussions, and to three anonymous reviewers for their valuable comments on the manuscript. F. E., I. S. and P. A. were funded through GLOMAR – Bremen International Graduate School for Marine Sciences (Grant no. GSC119) and supported by the DFG-Research Center/Cluster of Excellence, MARUM - The Ocean in the Earth System (Grant no. EXC309). P. A. was additionally supported by the Centre for Ice, Climate and Ecosystems (ICE) at the Norwegian Polar Institute.

Appendix A. Supplementary material

Supplementary data associated with this article can be found in the online version at http://dx.doi.org/10.1016/j.dsr.2014.04.007.

References

Armbrecht, L.H., Smetacek, V., Assmy, P., Klaas, C., 2014. Cell death and aggregate formation in the giant diatom *Coscinodiscus wailesii* (Gran & Angst, 1931). J. Exp. Mar. Biol. Ecol. 452, 31–39.

Assmy, P., Smetacek, V., Montresor, D., Klaas, C., Henjes, J., Strass, V.H., Arrieta, J.M., Bathmann, U., Berg, G.M., Breitbarth, E., Cisewski, B., Friedrichs, L., Fuchs, N., Herndl, G.J., Jansen, S., Krägefsky, S., Latasa, M., Peeken, I., Rottgers, R., Scharek, R., Schüller, S.E., Steigenberger, S., Webb, A., Wolf-Gladrow, D., 2013. Thick-shelled, grazer-protected diatoms decouple ocean carbon and silicon cycles in the iron-limited Antarctic Circumpolar Current. Proc. Natl. Acadl Sci. USA 110 (51), 20633–20638, http://dx.doi.org/10.1073/pnas.1309345110.

Assmy, P., Henjes, J., Klaas, C., Smetacek, V., 2007. Mechanisms determining species dominance in a phytoplankton bloom induced by the iron fertilization experiment EisenEx in the Southern Ocean. Deep-Sea Res. I 54, 340–362.

Blain, S., Quéguiner, B., Armand, L., Belviso, S., Bombled, B., Bopp, L., Bowie, A., Brunet, C., Brussaard, C., Carlotti, F., Christaki, U., Corbiere, A., Durand, I., Ebersbach, F., Fuda, J.-L., Garcia, N., Gerringa, L., Griffiths, B., Guige, C., Guillerm, C., Jacquet, S.H.M., Jeandel, C., Laan, P., Lefevre, D., Lo Monaco, C., Malits, A., Mosseri, J., Obernosterer, I., Park, Y.-H., Picheral, M., Pondaven, P., Remenyi, T., Sandroni, V., Sarthou, G., Savoye, N., Scouarnec, L., Souhaut, M., Thuiller, D., Timmermans, K., Trull, T., Uitz, J., van Beek, P., Veldhuis, M., Vincent, D., Viollier, E., Vong, L., Wagener, T., 2007. Effect of natural iron fertilization on carbon sequestration in the Southern Ocean. Nature 446, 1070–1075.

Boyd, P.W., Jickells, T., Law, C., Blain, S., Boyle, E.A., Buesseler, K.O., Coale, K.H., Cullen, J.J., de Baar, H.J.W., Follows, M., Harvey, M., Lancelot, C., Levasseur, M., Owens, N.P.J., Pollard, R., Rivkin, R.B., Sarmiento, J., Schoemann, V., Smetacek, V., Takeda, S., Tsuda, A., Turner, S., Watson, A.J., 2007. Mesoscale iron enrichment experiments 1993–2005: synthesis and future directions. Science 315, 612–617.

Boyd, P.W., Trull, T.W., 2007. Understanding the export of biogenic particles in oceanic waters: is there consensus? Prog. Oceanogr. 72 (4), 276–312.

Boyd, P.W., Watson, A.J., Law, C.S., Abraham, E.R., Trull, T., Murdoch, R., Bakker, D.C.E., Bowie, A.R., Buesseler, K.O., Chang, H., Charette, M., Croot, P., Downing, K., Frew, R., Gall, M., Hadfield, M., Hall, J., Harvey, M., Jameson, G., LaRoche, J., Liddicoat, M., Ling, R., Maldonado, M.T., McKay, R.M., Nodder, S., Pickmere, S., Pridmore, R., Rintoul, S., Safi, K., Sutton, P., Strzepek, R., Tanneberger, K., Turner, S., Waite, A., Zeldis, J., 2000. A mesoscale phytoplankton bloom in the polar Southern Ocean stimulated by iron fertilization. Nature 407 (6805), 695–702.

Buesseler, K.O., Boyd, P.W., 2009. Shedding light on processes that control particle export and flux attenuation in the twilight zone of the open ocean. Limnol. Oceanogr. 54 (4), 1210–1232.

Coale, K.H., Johnson, K.S., Chavez, F.P., Buesseler, K.O., Barber, R.T., Brzezinski, M.A., Cochlan, W.P., Millero, F.J., Falkowski, P.G., Bauer, J.E., Wanninkhof, R.H., Kudela, R.M., Altabet, M.A., Hales, B.E., Takahashi, T., Landrey, M.R., Bidigare, R.R., Wang, X., Chase, Z., Strutton, P.G., Friederich, G.E., Gorbunov, M.Y., Lance, V.P., Hilting, A.K., Hiscock, M.R., Demarest, M., Hiscock, W.T., Sullivan, K.F., Tanner, S.J., Gordon, R.M., Hunter, C. N., Elrod, V.A., Fitzwater, S.E., Jones, J.L., Tozzi, S., Koblizek, M., Roberts, A.E., Herndon, J., Brewster, J., Ladizinsky, N., Smith, G., Cooper, D., Timothy, D., Brown, S.L., Selph, K. E., Sheridan, C.C., Twining, B.S., Johnson, Z.I., 2004. Southern Ocean Iron Enrichment Experiment: carbon cycling on high- and low-Si waters. Science 304, 408–414.

Close, H.G., Shah, S.R., Ingalls, A.E., Diefendorf, A.F., Brodie, E.L., Hansman, R.L., Freeman, A., Aluwihare, L.I., Pearson, A., 2013. Export of submicron particulate

organic matter to mesopelagic depth in an oligotrophic gyre. Proc. Natl. Acad. Sci. USA 110, 12565–12570, http://dx.doi.org/10.1073/pnas.1217514110.
Corzo, A., Rodríguez-Gálvez, S., Lubian, L., Sangrá, P., Martínez, A., Morillo, J.A., 2005. Spatial distribution of transparent exopolymer particles in the Bransfield Strait, Antarctica. J. Plankton Res. 27, 635–646.
De La Rocha, C.L., 2007. The biological pump. In: Heinrich, D.H., Karl, K.T. (Eds.), Treatise on Geochemistry. Pergamon, Oxford, pp. 1–29.
Ebersbach, F., Trull, T., 2008. Sinking particle properties from polyacrylamide gels during the KErguelen Ocean and Plateau compared Study (KEOPS): zooplankton control of carbon export in an area of persistent natural iron inputs in the Southern Ocean. Limnol. Oceanogr. 53 (1), 212–224.
Ebersbach, F., Trull, T.W., Davies, D.M., Bray, S.G., 2011. Controls on mesopelagic particle fluxes in the Sub-Antarctic and Polar Frontal Zones in the Southern Ocean south of Australia in summer – perspectives from free-drifting sediment traps. Deep-Sea Res. II 58 (21–22), 2260–2276.
Gilron, G., Lynn, D., 1989. Assuming a 50% cell occupancy of the lorica overestimates tintinnine ciliate biomass. Mar. Biol. 103 (3), 413–416.
González, H.E., Mazzocchi, M.G., Giesecke, R., Borrione, I., Mahadik, G., Martin, P., Vandromme, P., Ribera d'Alcalà, M., Assmy, P., Iversen, M., Naqvi, W., Smetacek, V., In situ evidence of zooplankton control on phytoplankton growth and carbon export during the iron fertilization experiment LohaFEX in SW Atlantic ocean. in preparation.
Harvey, M.J., Law, C.S., Smith, M.J., Hall, J.A., Abraham, E.R., Stevens, C.L., Hadfield, M.G., Ho, D.T., Ward, B., Archer, S.D., Cainey, J.M., Currie, K.I., Devries, D., Ellwood, M.J., Hill, P., Jones, G.B., Katz, D., Kuparinen, J., Macaskill, B., Main, W., Marriner, A., McGregor, J., McNeil, C., Minnett, P.J., Nodder, S.D., Peloquin, J., Pickmere, S., Pinkerton, M.H., Safi, K.A., Thompson, R., Walkington, M., Wright, S.W., Ziolkowski, L.A., 2011. The SOLAS air-sea gas exchange experiment (SAGE) 2004. Deep-Sea Res. Part II: Top. Studies Oceanogr. 58 (6), 753–763.
Hillebrand, H., Dürselen, C.-D., Kirschtel, D., Pollinger, U., Tamar, Z., 1999. Biovolume calculation for pelagic and benthic microalgae. J. Phycol. 35, 403–424.
Hong, Y., Smith, W.O.J., White, A.-M., 1997. Studies on transparent exopolymer particles (TEP) produced in the Ross Sea (Antarctica) and by *Phaeocystis Antarctia* (Prymnesiophyceae). J. Phycol. 33, 368–376.
Jouandet, M.-P., et al., 2011. Optical imaging of mesopelagic particles indicates deep carbon flux beneath a natural iron fertilized bloom in the Southern Ocean. Limnol. Oceanogr. 56 (3), 1130–1140.
Kwon, E.Y., Primeau, F., Sarmiento, J.L., 2009. The impact of remineralization depth on the air-sea carbon balance. Nat. Geosci. 2, 630–635.
Lampitt, R.S., Achterberg, E.P., Andersom, T.H., Hughes, J.A., Iglesias-Rodriguez, M.D., Kelly-Gerreyn, B.A., Lucas, M.I., Popova, E.E., Sanders, R., Shepherd, J.G., Smythe-Wright, D., Yool, A., 2008a. Ocean fertilization: a potential means of geoengineering? Philos. Trans. R. Soc. A, 1–27 (published online).
Lampitt, R.S., Boorman, B., Brown, L., Lucas, M., Salter, I., Sanders, R., Saw, K., Seeyave, S., Thomalla, S.J., Turnewitsch, R., 2008b. Particle export from the euphotic zone: estimates using a novel drifting sediment trap, ^{234}Th and new production. Deep-Sea Res. Part I: Oceanogr. Res. Papers 55 (11), 1484–1502.
Lampitt, R.S., Noji, T., von Bodungen, B., 1990. What happens to zooplankton faecal pellets? Implications for material flux. Mar. Biol. 104, 15–23.
Ling, S.C., Alldredge, A.L., 2003. Does the marine copepod *Calanus pacificus* consume transparent exopolymer particles (TEP). J. Plankton Res. 25 (5), 507–515.
Lutz, M., Dunbar, R., Caldeira, K., 2002. Regional variability in the vertical flux of particulate organic carbon in the ocean interior. Glob. Biogeochem. Cycles 16 (3, 1037) (11/11-18).
Martin, J.H., 1990. Glacial–interglacial CO_2 change: the iron hypothesis. Paleoceanography 5 (1), 1–13.
Martin, P., Lampitt, R.S., Perry, M.J., Sanders, R., Lee, C., D'Asaro, E., 2011. Export and mesopelagic particle flux during a North Atlantic spring diatom bloom. Deep-Sea Res. I 58, 338–349.
Martin, P., Rutgers van der Loeff, M.M., Cassar, N., Vandromme, P., d'Ovidio, F., Rengarajan, R., Soares, M., Gonzalez, H.E., Ebersbach, F., Lampitt, R.S., Sanders, R., Barnett, B.A., Smetacek, V., Naqvi, S.W.A., 2013. Iron fertilization enhanced net community production but not downward particle flux during the Southern Ocean iron fertilization experiment LOHAFEX. Glob. Biogeochem. Cycles, 27, http://dx.doi.org/10.1002/gbc.20077.
Martiny, A.C., Pham, C.T.A., Primeau, F.W., Vrugt, J.A., Moore, J.K., Levin, S.A., Lomas, M.W., 2013. Strong latitudinal patterns in the elemental ratios of marine plankton and organic matter. Nat. Geosci. , http://dx.doi.org/10.1038/NGEO1757.
Menden-Deuer, S., Lessard, E.J., 2000. Carbon to volume relationship for dinoflagellates, diatoms, and other protist plankton. Limnol. Oceanogr. 45 (3), 569–579.
Michaels, A.F., Silver, M.W., 1988. Primary production, sinking fluxes and the microbial food web. Deep-Sea Res. 35, 473–490.
Mazzocchi, M.G. et al., in preparation. Mesozooplankton communites during the Lohafex iron fertilization experiment: Structural and functional responses in the epipelagic layer.
Noji, T.T., Estep, K.W., MacIntyre, F., Norrbin, F., 1991. Image analysis of faecal material grazed upon by three species of copepods: evidence for coprorhexy, coprophagy and coprochaly. J. Mar. Biol. Assoc. UK 71, 465–480.
Ortega-Retuerta, E., Reche, I., Pulido-Villena, E., Agustí, S., Duarte, C.M., 2009. Uncoupled distributions of transparent exopolymer particles (TEP) and dissolved carbohydrates in the Southern Ocean. Mar. Chem. 115, 59–65.
Parekh, P., Dutkiewicz, P., Follows, M.J., Ito, T., 2006. Atmospheric carbon dioxide in a less dusty world. Geophys. Res. Lett. 33 (L03610).
Passow, U., Alldredge, A.L., 1995. A dye-binding assay for the spectrophotometric measurement of transparent exoplomer particles (TEP). Linmol. Oceanogr. 40 (7), 1326–1335.
Passow, U., Alldredge, A.L., 1999. Do transparent exoplolymer particles (TEP) inhibit grazing by the euphausiid *Euphausia pacifica*? J. Plankton Res. 21, 2203–2217.
Passow, U., Kozlowski, W., Vernet, M., 1995. Palmer LTER: temporal variability of transparent exopolymer particles in Arthur Harbor during the 1994–1995 growth season. Antarct. J. U S 30, 265–266.
Passow, U., Shipe, R.F., Murray, A., Pak, D.K., Brzezinski, M.A., Alldredge, A.L., 2001. The origin of transparent exopolymer particles (TEP) and their role in the sedimentation of particulate matter. Cont. Shelf Res. 21, 327–346.
Pollard, R.T., Salter, I., Sanders, R.J., Lucas, M.I., Moore, C.M., Mills, R.A., Statham, P.J., Allen, J.T., Baker, A.R., Bakker, D.C.E., Charette, M.A., Fielding, S., Fones, G.R., French, M., Hickman, A.E., Holland, R.J., Hughes, J.A., Jickells, T.D., Lampitt, R.S., Morris, P.J., Nedelec, F.H., Nielsdottir, M., Planquette, H., Popova, E.E., Poulton, A.J., Read, J.F., Seeyave, S., Smith, T., Stinchcombe, M., Taylor, S., Thomalla, S., Venables, H.J., Williamson, R., Zubkov, M.V., 2009. Southern Ocean deep-water carbon export enhanced by natural iron fertilization. Nature 457, 577–580.
Richardson, T.L., Jackson, G.A., 2007. Small phytoplankton and carbon export from the surface ocean. Science 315, 838–840.
Rynearson, T.A., Richardson, K., Lampitt, R.S., Sieracki, M.E., Poulton, A.J., Lyngsgaard, M.M., Perry, M.J., 2013. Major contribution of diatom resting spores to vertical flux in the sub-polar north atlantic. Deep-Sea Res. Part I 82, 60–71.
Salter, I., Lampitt, R.S., Sanders, R., Poulton, A., Kemp, A.E.S., Boorman, B., Saw, K., Pearce, R., 2007. Estimating carbon, silica and diatom export from a naturally fertilised phytoplankton bloom in the Southern Ocean using PELAGRA: a novel drifting sediment trap. Deep-Sea Res. Part II: Top. Stud. Oceanogr. 54 (18-20), 2233–2259.
Schulz, I. et al., in prep. Response of a flagellate-dominated plankton community to artificial iron fertilization in the Southern Ocean. Deep-Sea Res. II: Top. Studies Oceanogr.
Smetacek, V., Klaas, C., Strass, V.H., Assmy, P., Montresor, M., Cisewski, B., Savoye, N., Webb, A., d'Ovidio, F., Arrieta, J.M., Bathmann, U., Bellerby, R., Berg, G.M., Croot, P.L., Gonzalez, S., Henjes, J., Herndl, G.J., Hoffmann, L.J., Leach, H., Losch, M., Mills, M.M., Neill, C., Peeken, I., Rottgers, R., Sachs, O., Sauter, E., Schmidt, M.M., Schwarz, J., Terbrüggen, A., Wolf-Gladrow, D., 2012. Deep carbon export from a Southern Ocean iron-fertilized diatom bloom. Nature 487, 313–319.
Smetacek, V., Naqvi, S.W.A., 2008. The next generation of iron fertiisation experiments in the Southern Ocean. Philos. Trans. R. Soc. Lond. A 366, 3947–3967.
Taucher, J., Oschlies, A., 2011. Can we predict the direction of marine primary production change under global warming? Geophys. Res. Lett. 38 (L02603).
Thiele, S., Fuchs, B.M., Ramaiah, N., Amann, R., 2012. Microbial community response during the iron fertilization experiment LOHAFEX. Appl. Environ. Microbiol. 78, 8803–8812.
Throndsen, J., 1995. Estimating cell numbers. In: Hallegraeff, G.M., M., A.D., Cembella, A.D. (Eds.), Manual on Harmful Marine Microalgae. UNESCO, Paris, pp. 63–80.
Turner, J.T., 2002. Zooplankton fecal pellets, marine snow and sinking phytoplankton blooms. Aquat. Microb. Ecol. 27 (1), 57–102.
Volk, T., Hoffert, M.I., 1985. Ocean carbon pumps: analysis of relative strengths and efficiencies in ocean-driven atmospheric CO2 changes. Geophys. Monogr. 32, 99–110.
Waite, A.M., Safi, K.A., Hall, J.A., Nodder, S.D., 2000. Mass sedimentation of picoplankton embedded in organic aggregates. Limnol. Oceanogr. 45 (1), 87–97.
Wassmann, P., 1998. Retention versus export food chains: processes controlling sinking loss from marine pelagic systems. Hydrobiologia 363, 29–57.
Wilson, S.E, Steinberg, D.K., 2010. Autotrophic picoplankton in mesozooplankton guts: evidence of aggregate feeding in the mesopelagic zone and export of small phytoplankton. Mar. Ecol. Prog. Ser. 412, 11–27.